Light to Sound: The Remote Acoustic Sensing Satellite (RASSat)

Dan Slater
Independent Consultant
La Habra Heights, CA; (562) 691-1987
dslater@ix.netcom.com

Rex Ridenoure
Ecliptic Enterprises Corporation
Pasadena, CA; (626) 278-0435
rridenoure@eclipticenterprises.com

Dave Klumpar
Montana State University
Bozeman, MT; (406) 579-9674
klump@physics.montana.edu

John Carrico
Independent Consultant
Sunnyvale, CA; (650) 253-5676
astrogatorjohn@gmail.com

Moriba Jah
University of Arizona
Tucson, AZ; (808) 269-4237
moribajah@email.arizona.edu

ABSTRACT

"*In space, no one can hear you scream*," as the tagline from the sci-fi film *Aliens* goes. But what if there were a way of "hearing" in space, moving in-space video from the Silent Era to a more contemporary cinematic experience? How could this capability be applied to shape future spacecraft and mission designs? Such a capability can be effectively incorporated into a 3U CubeSat using a measurement technique called Remote Acoustic Sensing (RAS). "RASSat" uses advanced optical sensors to view and recover audio from distant objects that have weak optical modulations produced by local sound and vibration sources; the modulated light sources and the RAS sensor are passively coupled at the speed of light, yielding a variety of interesting sounds across the entire human auditory range. RAS field demonstrations and analyses have identified and characterized terrestrial sound sources observable from LEO, along with associated acousto-optic modulation mechanisms. RASSat sensitivity is such that both day and night strong, easily detectable terrestrial acousto-optic emitters abound, and applications to Space Situational Awareness and planetary exploration are also evident. This paper provides an overview of the RAS measurement technique and recent terrestrial demonstrations, and highlights key RASSat design features, performance capabilities and applications.

INTRODUCTION

Electro-optical remote sensing satellites are increasingly able to provide high-resolution video observations of terrestrial activity. On orbit videos show the dynamic spatial and temporal characteristics of both cultural and natural activity. It would be interesting if these satellites could also remotely sense associated terrestrial acoustic activity. The fusion of visual and aural observations would improve an overall understanding of a scene and provide a more cinema-like viewing experience. A new technology, called Remote Acoustic Sensing (RAS), provides a potential pathway for acoustic observations of planetary surface activity from an orbiting spacecraft.

The first question is: would it even be technically possible to hear any terrestrial sounds from an orbiting spacecraft? As is well known, sound -- the brain's interpretation of a modulated frequency sensed by the human ear with air particles being the carrier -- does not propagate through a vacuum. In a vacuum, air is absent but photons can carry an equivalent information content. The ear cannot sense photons, but optical signals can be converted into an equivalent acoustic signal, which is termed here as an acousto-optic signature. (We use this term rather than the more typical "photoacoustic" because fundamentally RAS relies on sound-to-light-to-sound conversion vs. light-to-sound.)

RAS, as applied herein to the RASSat concept, is a form of a distributed microphone system that separates an acoustic sensor into two (or more) spatially separated elements: a naturally formed in situ terrestrial acousto-optic modulator (AOM) and a space-based remote readout sensor. RAS does not require acoustic wave propagation in space but instead passively couples the AOM to the readout sensor over orbital distances using ambient light fields[1,2]. Acoustic wave propagation is only required between the sound source and the in situ AOM and not to the readout sensor.

RAS can be implemented in a variety of ways. But in general RAS relies on an acoustically or mechanically excited object modulating light or other electromagnetic energy, which is then remotely sensed. One form of optical RAS is an enhanced modern-day derivative of the Photophone originally invented by Alexander Graham Bell in 1880[3,4,5,6,7] (see Fig. 1). Bell set up a speaking tube next to a thin shiny membrane that was reflecting sunlight to a distant parabolic mirror with a Selenium photocell and headphones. Acoustic vibration of the membrane weakly modulated the sunlight intensity which was then recovered by the photocell and headphones at a 213-m (700-foot) distance. Bell considered the Photophone to be his most important invention -- even more important than the telephone -- but the rest of the world thought otherwise and generally forgot about it.

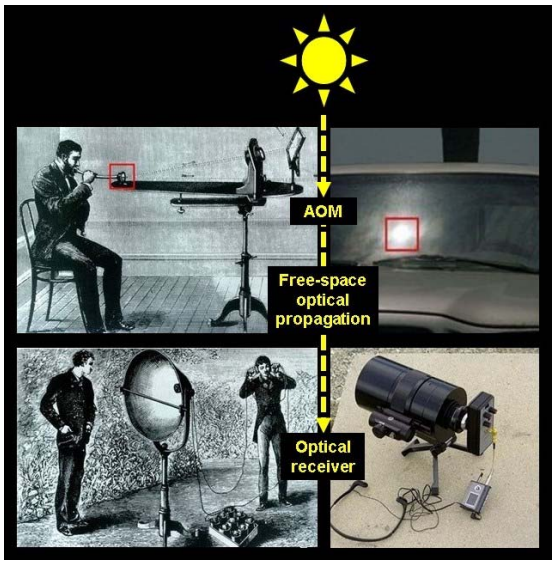

Fig. 1. Comparison between Bell's 1880 Photophone (l) and 2006 RAS technique (r). The Photophone demonstrated a link over ~0.2 km (~700 feet); the 2006 RAS worked at over 40 km (25 miles).

As shown in Fig. 1, in Bell's setup the membrane, illuminated by both the Sun and the speaker's voice, is an AOM. We extend the Photophone concept by using naturally existing in situ membrane AOMs such as preexisting windows, thin shiny surfaces and vehicle skins. Two optical and one acoustic propagation links (AOM illumination source, AOM acoustic source and AOM-to-optical receiver) are simultaneously required for this RAS variant to work. RAS can also be extended to stereophonic and multichannel sound by using multiple distributed in situ AOMs, and when combined with high-definition video it holds the potential to provide a cinema-like immersive viewing experience.

RAS DEVELOPMENT (2006-PRESENT)

The Photophone AOM variant is one of a variety of RAS optical sound-modulation mechanisms[2]. Observing flames, rocket plumes, lightning and other self-luminous acoustic emitters uses a different AOM

mechanism. Turbulent flow within a rocket plume results in a propagating audio frequency pressure wave (the definition of sound). The pressure fluctuations are directly associated with audio-frequency luminosity variations which are observable by the RAS photoreceiver. Multiple plume locations can be observed, corresponding to multiple microphone locations. We have observed rocket plumes with multiple RAS spatial channels demonstrating the stereophonic capability.

The bright flash of a lightning discharge produces a strong optical signal that corresponds to a local pressure surge at the discharge location. Fireworks behave in a similar manner, and we have observed these with stereophonic RAS. It is quite interesting to look at distant fireworks and simultaneously hear the associated sounds with stereophonic localization and with perfect visual/aural synchronization. Self-luminous acousto-optic sources produce some of the strongest terrestrial RAS signals and will be important observational targets for RASSat due to their signal strength and prevalence.

Most researchers have used high-speed video cameras (1,000 to 20,000 frames per second) as AOM readout devices followed by various forms of software-intensive image analysis such as extracting the local surface motion vectors of arbitrary scattering surfaces[8,9,10]. We instead primarily use low pixel-count photoelectric readout sensors with a very wide dynamic range (up to 24 bits) and very high sample rates (up to 48 KHz) and have combined this with a diversity of optics and AOM methods. Although the lead author has also worked with radio-frequency RAS variants[2], this paper only considers optical implementations.

RAS experiments performed by the lead author (Fig. 2) over the last 10 years have demonstrated the ability to visually and aurally observe a variety of scenes ranging from exoatmospheric rocket flight at >100 km observing distances, ground-based visual / aural observations at 45 km (28 mile) distances to extreme close-up views of protozoa within micro-aquatic worlds [1,2,11,12,13]. The long-range rocket and terrestrial observations are of particular interest as they provide a foundation for orbital RAS.

This paper, as a continuation of this earlier RAS work, explores the RAS methodology needed for listening to planetary surface acoustic activity from an orbiting spacecraft. We first summarize desired top-level mission and system requirements for RASSat, and

Figure 2. The lead author conducting RAS field tests in 2015 during the Space Launch System QM-1 solid-rocket booster static firing test at the Orbital ATK plant in northern Utah.

then discuss some of the easier-to-observe terrestrial acoustic sources along with the associated acousto-optic modulation mechanisms. We then describe and show results from a ground-based simulation system using scaled optics to observe nearby terrestrial scenes with suitably attenuated signal levels that correspond to on-orbit views. Next we describe a RAS technology demonstrator payload and show how to integrate it into the 3U RASSat. This is then followed by a discussion of a possible RASSat demonstration mission.

RASSAT MISSION AND SYSTEM OBJECTIVES

While the relatively new RAS technology has been proven through multiple ground-based field operations since 2006, it has never been applied to remote sensing from space. RASSat could thus serve as a proof-of-concept demonstration mission to inform future RAS-oriented spacecraft and mission designs and related applications.

Key objectives of the initial RASSat mission (and associated rationale) are:

- Demonstrate RAS capability from LEO against a number of natural and human-made targets on the Earth's surface or in its atmosphere (provides a representative sample of likely terrestrial phenomena to observe and evidence of relevance and usefulness to the respective communities interested in such phenomena).

- Demonstrate RAS capability from LEO against a number of space-based targets (provides evidence of relevance and usefulness to Space Situational Awareness community, SSA).
- Ground tracks shall cover a sufficient range of latitudes with precession in local time over a mission duration of several months to permit RAS observations over a range of solar illumination angles (provides adequate observational parameters to validate overall RAS effectiveness).
- The orbit inclination shall be large enough to cover a range of land and water terrains including high population-density regions (provides adequate sampling of urban, rural/remote and ocean targets).
- Conduct mission operations for 3-9 months (would provide for adequate time to complete demonstrations while keeping total mission cost in check).

Related top-level RASSat spacecraft system objectives include:

- Demonstrate that an effective RAS payload can be incorporated into a standard 3U CubeSat platform (provides evidence of relevance and usefulness to burgeoning CubeSat ecosystem and keeps total system cost in check).
- Demonstrate that readily available CubeSat subsystems adequately support effective RAS observations (keeps non-recurring engineering and total mission cost in check, and enhances overall system reliability).
- Capitalize on existing cost-effective capabilities for launching RASSat into LEO and for conducting mission operations there (keeps non-recurring engineering and total mission cost in check).

This simple set of top-level requirements are adequate enough to allow for a compelling RASSat mission and system design. Understanding the next level of technical detail, especially the design and performance requirements for the RAS payload module and various spacecraft subsystems, hinges on understanding the range of observable RAS targets. Fortunately, much can be learned in this regard from ground-based situations which simulate LEO-based performance.

The RASSat Payload Simulator

To better understand terrestrial acoustic observability from an orbiting spacecraft we fabricated a RAS Simulator (RASSIM). The simulator used baseline visual and aural RASSat sensor hardware but with a much smaller optical aperture and focal length to reduce the received optical signal to what it would be at RASSat orbital distances. The aperture and focal length scaling produces fields of view and signal levels at 5- to 20-km distances comparable to those observable from a RASSat in a 400-km LEO orbit.

RASSIM includes both full focal length and scaled aperture and focal length imagers and RAS detectors. The full focal length imager and RAS detector is intended to view scaled test objects and also supports RASSat optics development. The full focal length imaging telescope operates at 500 mm f/6.2. The scaled focal length imager and RAS detector views full-scale objects from scaled orbital distances and is used to evaluate on-orbit observability. The scaled focal length imaging telescope operates at 25 mm f/6.2 to reduce the viewing distance by a factor of 20. In other words, viewing an object at a distance of 20 km with the scaled optics would be equivalent to an on-orbit observation from a 400-km viewing distance. Other scaled lens focal lengths and apertures are also used to change the observing scale factor as appropriate.

RASSIM uses a small-aperture RAS receiver with lens entrance pupil diameter scaled by the test view to orbital-view distance. For example, according to the inverse-square law, observing a scene with a 0.8-mm aperture telescope at a 16-km distance would produce a similar signal level as an 80-mm aperture telescope at a 1600-km distance. The 81-mm aperture RASSat telescope uses a 500-mm focal length. The simulator uses a 25-mm focal length variable aperture lens.

A variety of natural and cultural scenes of opportunity were observed with the RASSIM under both day and night conditions. Example naturally occurring phenomena include lightning, water/air surface interactions (wave heights and surface roughness), erupting volcanos, ice flows, etc. Cultural phenomena include various types of lighting, flames and flares, etc.

When possible we determined the scene distance and roughly recorded the RAS signal quality. Using these two parameters we created a crude on-orbit RAS observability table as shown in Table 1. The results are approximate but they do suggest that some terrestrial acoustic observations would be viable from LEO. The strongest terrestrial signals generally involve flames, pyrotechnics, fireworks and lightning. There are many

caveats, including for example that our observations were primarily horizontal while satellite observations are generally downward (vertical). Optical emissions from vehicle lights, beacons and many other light sources are generally directed at low elevation angles so detectability for those would likely be worse than shown here.
The small RASSat CubeSat acoustic sensitivity is relatively low but there are strong easily detectable terrestrial acoustic emitters, both day and night. So far, the strongest acoustic signals have been associated with high energy acousto-optic emissions including lightning, rocket plumes, flames and even Disneyland fireworks displays (see Fig. 3). Solar glinting objects, as a variation of the Bell Photophone, provide another potentially observable acousto-optic modulation mechanism. Additionally there are interesting non-acoustic yet audio frequency-modulated optical emitters observable from orbital distances including city AC lighting and aircraft beacons. RASSat could also observe vibrations and acoustic energy produced by itself, the launcher and other glinting spacecraft such as the International Space Station (ISS).

The ground-based RAS experiments related RASSIM work have shown that meaningful LEO satellite demonstrations could be performed cost effectively with a 3U CubeSat. At the top level, RASSat is generally similar to other small remote-sensing satellites such as the Planet Labs Dove series but with the addition of the acoustic detection capability. Several RAS payload sensor architectures were evaluated before selecting a shared-aperture telescope using separate imaging and acoustic readout sensors, as summarized next.

RASSAT SENSOR PAYLOAD

Especially for the first RASSat spacecraft (baselined here as a technology demonstrator), there is strong interest in having the sensor payload consist of a variety of RAS-based sensors rather than just one, plus a quality imaging capability to provide context for the RAS observations. It is also of interest to consider having an intermediate RAS demonstrator sensor package onboard the ISS someday, either in series with or parallel to the RASSat project. Ideally, the overall optical design and packaging of this ISS version should be close to that planned for RASSat. Finally, to keep development costs low it's desirable to employ commercially available optical equipment for all ground-based lab and field work.

Overall Telescope Design

RASSat is a remote-sensing satellite that views the Earth both visually and aurally at moderate resolution. Like other similar electro-optical remote-sensing 3U CubeSats, RASSat includes a telescope with various focal plane sensors, in this case a CMOS imager (for the context imaging) and several RAS detectors. Several RAS sensor payload architectures were evaluated before selecting a shared-aperture telescope design using separate imaging and opto-acoustic sensors. The imaging performance for such a system is in the range of <10-m Ground Sample Distance (GSD). Additional driving RASSat telescope requirements include an aperture at least 80 mm in diameter as needed to achieve the desired ~10-m ground resolution (but <100 mm so it can fit comfortably within the 1U cross section) and a focal length that provides optimal spatial sampling, high-quality imagery along with visible and NIR spectral compatibility (while still fitting comfortably within a 3U length).

Starting with the end goal of space-grade optics, two telescope options were considered: one employing a space-modified Commercial Off-The-Shelf (COTS) lens (two variants were assessed) and an alternative design incorporating a custom low-mass, radiation-tolerant telescope design. High-quality imagery has already been demonstrated with the COTS telescopes; the custom design will have even better optical performance. These three options are compared in Table 2.

For the COTS option, the nearest equivalent readily available CubeSat-sized space telescope assembly is the high-quality 89-mm aperture space-rated Questar Maksutov telescope, as was used by the original Planet Labs Dove 3U CubeSats and also by other rocket and space-based systems[14,15]. The Dove Questar telescope uses a combination of a Cervit primary mirror and either an Invar housing or a composite truss to provide focus stability. The Dove satellites provide imagery in the 3- to 5-m resolution class[16]. One disadvantage of the Questar telescope is its length, taking up much of a 3U CubeSat volume. For RASSat, we opted to design a telescope around a COTS lens instead: a Nikon 500-mm f/8 N mirror lens with an 81-mm aperture. Although this particular Nikon mirror lens is no longer made it is high-quality and easy to find in the used camera marketplace. Even though the lens is

Table 1. On-orbit RASSat observability based on variable-aperture RASSIM terrestrial observations.

Scene	Scene Distance	Day	Night	Notes
Lightning storms	14 km / 80 km	560 km (strong)	3200 km (strong)	Very strong RAS emitter
Fireworks	16 km / 16 km	640 km (strong at dusk)	640 km (strong)	Very strong RAS emitter
City lights	6 km / 20 km	240 km (weak)	800 km (strong)	Strong 50/60 Hz and harmonics
Stadium lights	18 km / 18 km	720 km (weak)	720 km (strong)	Anaheim stadium, dusk
Radio tower beacon	11 km / 11 km	440 km (strong)	440 km (strong)	KFI radio tower (large beacon)
Aircraft in flight	2 km / 25 km	80 km (strong)	1000 km (moderate)	Xenon beacons, lights, solar glints
Automobiles	3 km / 6 km	120 km (weak)	240 km (moderate)	Head lights, tail lights, solar glints
Emergency vehicles	/ 4 km	Possible	160 km (weak)	Assumes upward emission
Large LED sign	/ 18 km	?	252 km (weak)	Sounds change with picture
Forest & building fires	6 km /	7 km (brush fire - weak)	?	Flames are strong RAS emitters

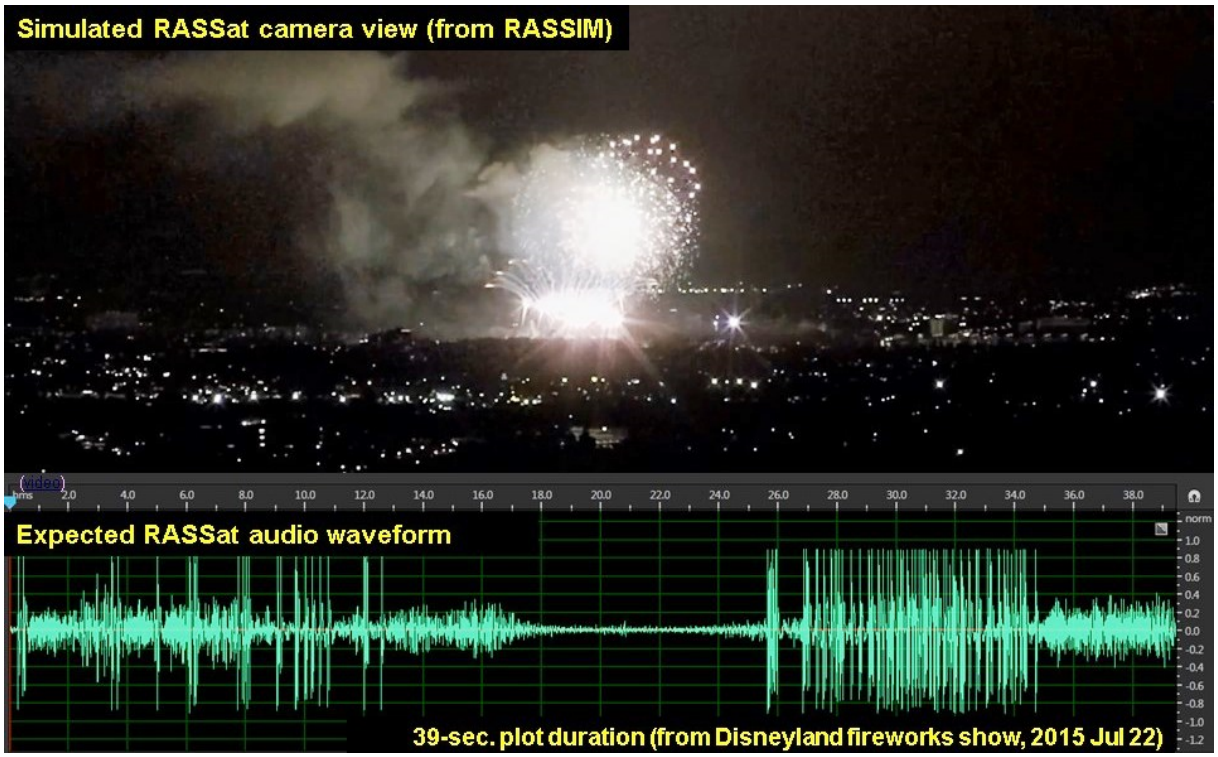

Fig. 3. Fireworks are a very strong opto-acoustic emitter and should be easily detectable in LEO by RASSat. This image shows the expected on-orbit visual and aural results for the proposed RASSat using the baseline sensors. Imagery was acquired from a 16-km (10-mile) distance using a 25-mm f/8 lens on a modified GoPro 4B camera and a 25-mm f/16 lens on the RAS detector.

Table 2: Small telescopes suitable for use in remote-sensing CubeSats. This table compares a Nikon 500-mm type-N COTS mirror lens with the proposed custom RASSat telescope lens. Also shown is a high-quality Questar telescope as used by the first- and second-generation Planet Labs Dove CubeSats. Note: The Nikon lens is capable of 42-mm image circle but with reduced performance.

Parameter	Nikon COTS	RASSat custom	Questar
Aperture	81 mm (measured)	81 mm (specification)	89 mm (specification)
Central obscuration	38 mm (measured)	24 mm (design)	31 mm (measured)
Focal length	500 mm (specification)	500 mm (specification)	1140 mm (Dove ref)
f-number	6.2 (calculated)	6.2 (calculated)	12.5 (calculated)
t-number	8 (specification)		
Focal region diameter	8 mm (RASSat requirement)	8 mm (specification)	>8 mm
Wavelength	Visible / near infrared	400 - 900 nm (specification)	Visible / near infrared
Resolution	Near diffraction limited (measured / calculated)	Diffraction limited	Diffraction limited
Illumination uniformity	>98% (calculated)	>97% (calculated)	
Geometric distortion	<0.4% (calculated)	<0.5% (calculated)	
Thermal control	None (refocus is needed)	Athermalized design	Cervit / Invar / composites
Radiation environment	Several months LEO (estimated)	8 years LEO (estimated)	>3 year LEO mission
Maximum mechanical diameter	90 mm (measured)	90 mm (estimated)	
Optical length (front vertex to focal plane)	142 mm (calculated)	113 mm (calculated)	320 mm (Dove ref)

specified as f/8 it actually is an f/6.2 optical design although with a t/8 light loss. The f/6.2 aperture provides good spatial sampling (2.5-m GSD at 400-km range) when using a 1.55-micron pixel size sensor typical of GoPro and many other small modern imaging sensors. The optical performance of this lens is excellent when using only the central 8-mm diameter region of the 42-mm diameter focal plane.

The optical model for this lens is described in US patent 4,666,259[17], which was then mathematically modeled using Zemax optical-design software. We also evaluated actual imagery acquired using this lens coupled to a modified GoPro camera and found it to perform close to the predicted performance expectations. We decided to use various low-cost, readily available COTS telescopes for prototype RAS sensor and support equipment development, RAS ground-truth field experiments, technology demonstrations and education, and RASSat breadboard development. Optical modeling of such designs is also relatively easy. If sufficiently modified, such telescopes could also be used for ISS-based experiments and possibly even in a CubeSat design.

For the custom RASSat telescope option, a Corrected Dall Kirkham (CDK) design was selected; most performance metrics for this option are better than the COTS design with the penalty of longer development schedule and higher cost. The basic CDK telescope uses an elliptical primary mirror with a spherical secondary mirror, and provides excellent on-axis performance but degrades elsewhere. The spherical secondary mirror simplifies manufacturing while also improving mechanical stability and alignment ease. The addition of a two-element refractive optical corrector using radiation-tolerant glasses corrects the

off-axis performance to provide a fully diffraction-limited focal plane. In optimizing the optical design we worked to minimize size, mass and thermal sensitivity while providing diffraction-limited performance. This custom telescope design has an identical aperture and focal length to the COTS telescopes but with a smaller overall envelope, less mass, better optical performance, better mechanical stability and a degree of resilience to space-radiation effects.

For most ground uses and ISS interior operation telescopes such as these can be readily refocused when needed. But focusing the telescope in a CubeSat is more difficult. If the focus drift is fast and large, it is not practical to keep the telescope in focus. A better approach is to athermalize the telescope using a combination of optical material selection, structure design and active and/or passive temperature control. The Questar space telescopes use low-CTE materials including Cervit, Fused Silica and Invar (carbon fiber and titanium in later versions). For the space-grade COTS and custom CDK telescope designs low-CTE reflectors and structural materials would be used, combined with passive thermal focus compensation and control. Having a mechanical focus trim capability is also prudent. The COTS Nikon and custom telescope options are at Technology Readiness Level (TRL) 3 and still require additional mechanical design work, engineering for athermalization, tolerance analysis and manufacturability engineering.

Optical Design and Sensor Layout

As shown in Fig. 4, the telescope output passes through a visible/near infra-red (NIR) dichroic cube beamsplitter to a pair of focal regions. The custom RASSat telescope design compensates for the spherical aberration that a cube beam splitter would normally introduce into the telescope output beam. A 12.5-mm cube beamsplitter was selected over a thin plate or pellicle beamsplitter for reasons of mechanical robustness and, in the case of the thin plate, easier-to-control optical aberrations. (COTS 12.5-mm beamsplitter cubes are available for supporting breadboard, qualification, educational and other related uses.)

The straight-through beam is to the color 1/2.3" CMOS imaging sensor. The right-angle NIR beam passes to several RAS sensors and LEDs. Key optical characteristics of the various sensors and detectors are summarized in Table 3.

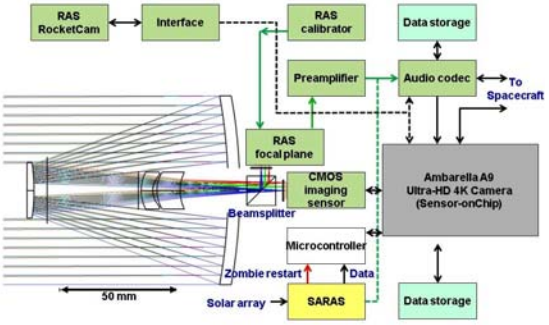

Fig. 4. RASSat payload block diagram. Core to the design is an 81-mm aperture Corrected Dall-Kirkham (CDK) telescope with 500-mm focal length and f/6.2 lens. The fully integrated payload module would occupy a volume of ~1.5U.

As was the case with the telescope, we also decided to find a COTS imager for RASSat that would be easy to use for the numerous ground support-related activities and for possible use in orbit. A modified GoPro camera is baselined. A useful ground-test version of the RASSat main telescope consists of nothing more than the Nikon 500-mm mirror lens coupled directly to the modified GoPro camera, as shown in Fig. 5.

Fig. 5. COTS telescope and camera in ground-test configuration.

These GoPro cameras provide a compact and fully self-contained imaging system including video capture, video image storage, RAS audio recording, LCD image viewing and configuration setup along with internal battery power storage. The GoPro can also simultaneously output standard-definition RS-170A and high-definition HDMI video with resolutions up to 4K at 30 frames per second. The GoPro camera is compatible with external remote control. At minimum, the modification requires removing the original fisheye lens. If baselined for use in space, significant additional mass, material, thermal

Table 3. RASSat main telescope geometry. (Assumptions: 400 km slant range, D = 81-mm aperture diameter, f = 500-mm focal length, λ = 0.5-micron, 1/2.3" sensor.)

Image format	1080p wide	1080p narrow	4K	RAS
Horizontal pixels	1920 = 5.952 mm	1920 = 2.976 mm	3840 = 5.952 mm	2 = 2 mm
Horizontal field of view	0.682° = 4762 m	0.341° = 2381 m	0.682° = 4762 m	0.229° = 1600 m
Vertical pixels	1080 = 3.348 mm	1080 = 1.674 mm	2160 = 3.348 mm	2 = 2 mm
Vertical field of view	0.384° = 2678 m	0.192° = 1339 m	0.384° = 2678 m	0.229° = 1600 m
Diagonal field of view	0.783° = 5463 m	0.391° = 2731 m	0.783° = 5463 m	0.324° = 2263 m
Pixel size (d)	3.10 μm	1.55 μm	1.55 μm	1000 μm
Ground Sample Distance (GSD)	6.2 μrad = 2.48 m	3.1 μrad = 1.24 m	3.1 μrad = 1.24 m	1571 μrad = 800 m
FWHM (1.03λ/d)	6.4 μrad = 2.5 m	6.4 μrad = 2.5 m	6.4 μrad = 2.5 m	6.4 μrad = 2.5 m
Airy disk (2.44λ/d)	15.1 μrad = 6.0 m	15.1 μrad = 6.0 m	15.1 μrad = 6.0 m	15.1 μrad = 6.0 m
Sampling density (fλ/d)	0.99	1.99	1.99	0.003

and electromagnetic compatibility modifications would be required. Ecliptic Enterprises Corporation has considerable experience with modifying COTS cameras for use in space[18], so other options are also available.

The right-angle beam splitter port (see Fig. 4) illuminates several photosensors that provide the RAS capability. The primary RAS photodetector is a 2x2 pixel Silicon photodiode with 1-mm pixels centered in the focal plane. We may also add several other RAS photosensors if we can fit them into the focal plane. Compared to conventional imagers and radiometers, the RAS photoreceivers are optimized for detecting very weak low-level audio-frequency modulations present on a strong optical carrier. We are also interested including an audio frequency-modulated focal plane LED with relatively high optical gain and directivity for simple downlink experiments. This would support simple low data-rate non-laser optical downlink experiments.

Fig. 4 also shows RAS interface electronics, which provide signal conditioning and sensor calibration. A Sun protection shutter may have to be added, but this has not yet been decided.

The RASSat payload also includes a small developmental version of an Ecliptic RAS RocketCam™, a very compact wide-angle video camera with stereophonic RAS capability. This provides a limited backup in case of failure of the main RASSat telescope. Other applications for this sensor include use as a star camera and for sensor space qualification in support of other projects. The camera is a Sony FCB-MA130 providing a 53° horizontal field of view with 1080p video and still images up to 13 Mpixel resolution. An engineering development version of the RAS RocketCam is currently operational (TRL 5) but using a GoPro camera instead.

Another important RAS-based technology to be demonstrated on RASSat is Solar Array Remote Acoustic Sensing (SARAS), which is isolated and separated from the primary RAS payload. SARAS uses the existing spacecraft solar power arrays to form large-area RAS detectors. The solar array parasitic capacitance generally limits the frequency response to audio frequencies, but the solar array otherwise can be quite sensitive to audio-frequency light-intensity fluctuations. SARAS consists of power-scavenging electronic circuitry connected directly to the solar arrays along with the electronics that extract the multichannel audio signals.

SARAS viability (TRL 4) has been demonstrated by a series of terrestrial RAS observations using a 1 ft^2 spacecraft silicon solar array test panel with power scavenging. Very strong RAS signals were obtained from a lighting storm at a 80-km (50-mile) distance (Fig. 6), and an Atlas V rocket launch and several fireworks displays were very easily detected at a 16-

km (10- mile) distance. A variety of day and night cultural activity has been observed using SARAS in terrestrial environments, some of which may be detectable from orbital distances. SARAS audio-frequency transfer function measurements have been performed with both Silicon and multi-junction solar cells.

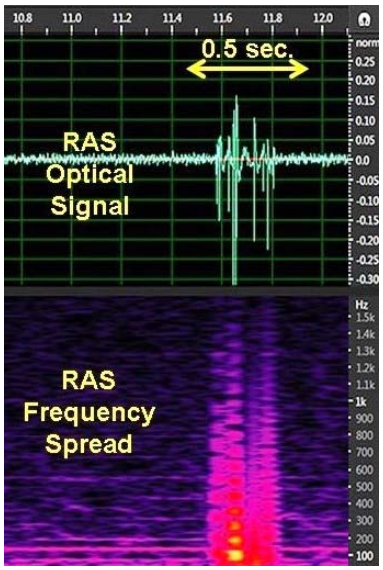

Fig 6. SARAS detection of a lightning storm at 80-km (50-mile) distance.

SARAS provides some interesting capabilities. The solar-array detector surface area is large and is already present on many spacecraft. We believe that it is likely that a variety of strong audio-frequency modulated terrestrial sources will be detectable from LEO altitudes.

Besides RAS detection, solar power arrays with SARAS hold the potential to be used for attitude determination, both day and night, and to receive low data-rate uplinks from distant lasercom transmitters. Solar arrays have been used for daytime attitude determination by looking at the array current flow[16]. But night time attitude determination may also be possible by detecting city lights (60 Hz) and lightning storm impulse activity. SARAS may also prove useful for Space Situational Awareness (SSA) and Rendezvous and Proximity Operations (RPO) as a tool for detecting internal and nearby satellite vibrations such as antenna deployments and thruster firings, nearby glinting space debris along with the presence and characterization of rendezvous and inspector satellite activity. Refueling leaks, bearing vibrations and other activity could potentially be aurally detected during on-orbit servicing. There are also some interesting acoustic detection possibilities using SARAS on planetary rovers related to weather and geophysical phenomena.

Adding SARAS capability to a spacecraft requires the addition of a relatively simple solar array interface module, as depicted in Fig. 7. This module connects directly to the solar arrays and outputs the recovered audio signal. As part of this, the SARAS interface can directly and independently scavenge DC power from the solar array. The SARAS interface power requirements are low and tend to be radiation-tolerant due to relatively simple circuitry and low data rates. The SARAS interface can be extended to include an independent tone or other audio decoder to extract a low bit-rate digital uplink from a terrestrial or space-based modulated laser. The resulting low data-rate command uplink can be used for general use. One interesting example is to provide a simple way to command solar-powered tumbling nano- or picosats while also eliminating the need for antennas, receivers and other RF command-uplink hardware. This would be of even more interest with laser-propelled spacecraft such as the proposed "Breakthrough Starshot" project. Because SARAS can be self-powered, uses simple robust circuitry and provides an independent uplink capability for a tumbling spacecraft, this technology may be useful for recovering 'zombie' satellites in which the normal RF command uplink, power subsystem or flight controller has failed.

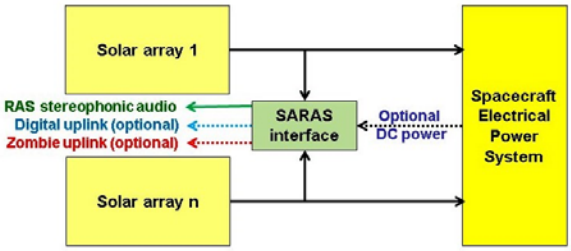

Fig. 7. SARAS block diagram.

The recent 2015 Lightsail-A and upcoming 2017 Lightsail-2 3U CubeSat missions could have been an interesting and ideal test case for demonstrating SARAS technology. Ecliptic is the prime contractor for both LightSail CubeSats, a private effort that is entirely funded by members and donors of The Planetary Society[19]. Each LightSail spacecraft is outfitted with a square-shaped, four-quadrant 32 m^2 deployable solar sail system. LightSail A was launched into low Earth orbit May 2015 for a 24-day

mission. After a flight computer crash and reboot, the CubeSat was finally able to deploy its solar sail, which increased drag causing the satellite to reenter the Earth's atmosphere several days later. LightSail 2 is scheduled for launch in early 2017.

The addition of a SARAS interface and audio downlink to the Lightsail CubeSat could have provided additional acoustic information in an audio bandwidth downlink channel. The large solar-illuminated solar sail can alternately be considered to be very large and extremely sensitive microphone membrane. Solar membrane glints along with terrestrial night activity could have supported a variety of SARAS experiments. Solar sail deployment sounds would have been heard, with sunlight or self-illuminated glints modulated by audio-frequency resonances, binding, stiction, motor pulses and other mechanical phenomena. Any audio frequency flutter or vibration of the large solar sail membrane has the potential to produce RAS-detectable optical modulations. With stereophonic sensing by using different solar sail quadrants, particular regions on the sail producing specific sounds can be localized. After the solar sail membrane deployment it's possible that micrometeorites, space dust or solar-wind impacts may be audible, followed later by a variety of stereophonic sounds during the atmospheric reentry process. The RAS audio can be compressed and downlinked in a much narrower bandwidth than video using amateur radio technology to provide wide real-time geographical coverage. In the case of spacecraft, meteor or other high-speed atmospheric re-entries, it is likely that plasma audio frequency-modulated optical and radio emissions would also be present and would be detectable using either optical or RF RAS techniques.

During the Lightsail A mission, the flight control computer failed due to a software bug[19]. The spacecraft then became a zombiesat, as there was no way to reboot the flight control computer. Fortunately a random cosmic ray hit a few days later did eventually reboot the computer, allowing the mission to continue. SARAS, with its simple electronics powered directly and independently by the solar array, may provide a useful alternative to reset the flight computer, the electrical power system or a RF communications uplink. Here, a ground-based audio-frequency modulated laser could have been used to command the spacecraft reset. The Lightsail A solar arrays are illuminated over a wide range of angles so a reboot command may be possible even while the spacecraft is rapidly tumbling.

RASSAT SPACECRAFT DESIGN

The RASSat spacecraft bus evolves from a series of 3U CubeSats developed at Montana State University (MSU) including the successful TRL-9 (1.5U) FIREBIRD bus currently delivering orbital measurements of relativistic electrons in support of its NSF mission[20] and the IT-SPINS bus currently in development[21]. An overview of the RASSat spacecraft interconnect architecture between the bus, RASSat sensor payload, and attitude control elements is shown in Fig. 8. The RAS sensor payload interfaces to the spacecraft for data handling and for receiving switched, regulated power, via the Payload Interface Board (PIB). Spacecraft systems support pointing control and knowledge via the Attitude Determination and Control (ADCS) subsystem. Power collection, conditioning and storage is handled by the Electrical Power System (EPS). A GPS receiver provides position and absolute timing.

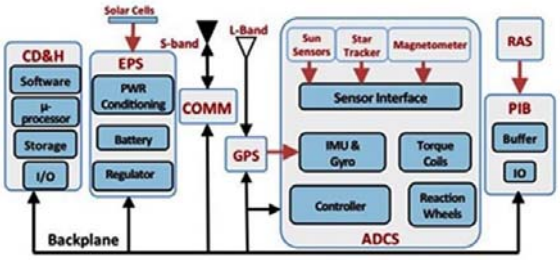

Fig. 8. RASSat block diagram.

These subsystems are integrated into a mechanical structure as a dynamically-balanced 3U spacecraft with star tracker, dual Sun sensors, and a UHF (or S-band) antenna deployed perpendicular to the 3-axis stabilized nadir-pointing spacecraft. The physical layout of the spacecraft is shown in Figs. 9 a, b and c, and brief descriptions of each subsystem follow.

Mechanical Subsystem

RASSat is fully compliant with the Cal Poly 3U CubeSat design specification, and is designed for deployment compatibility with the most commonly used CubeSat carrier/deployer systems. The primary RASSat spacecraft structure consists of a 3U CubeSat solid-wall structure, e.g. from Pumpkin (modified for RASSat). Standard mounts from the supplier will be used to mount the spacecraft subsystem elements. Custom mounts and cut-outs will be designed and built at MSU for the sensor payload module and UHF

dipole deployer. Sufficient interstitial volume and mass margin will be provided to accommodate the addition of vernier mass elements during static spacecraft load balancing. Other than the twin 'carpenter's ruler' UHF dipole antennas, no deployables are required. Antennas are stowed during launch in an external wrap-around configuration and restrained by a nylon filament which is severed by melting upon autonomous operation once deployed a safe distance from the carrier/deployer system.

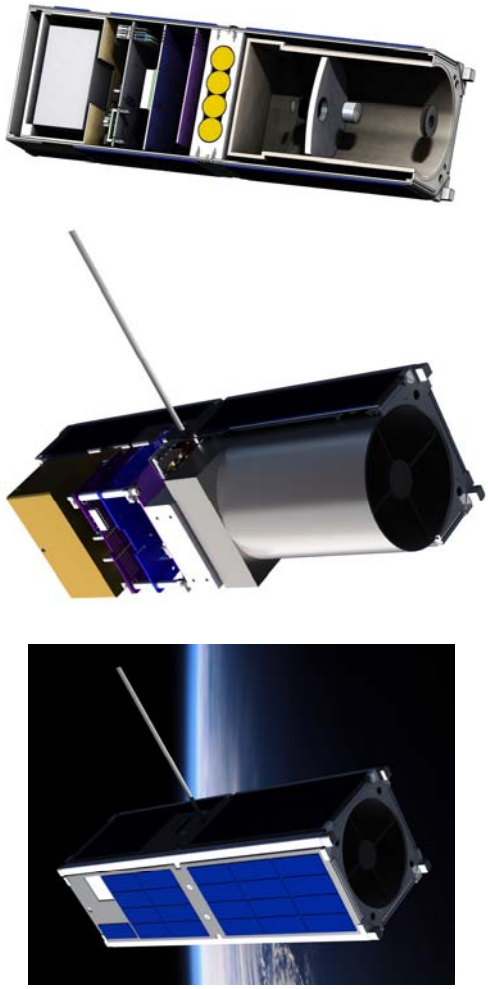

Fig. 9 a, b and c. RASSat spacecraft (cutaway and fully integrated views).

Command and Data Handling Subsystem (C&DH)

At the heart of the spacecraft bus is the CD&H system, which includes dual 32-MHz microchip PIC-24 processors, and 8GB of non-volatile flash memory for bus data, payload data, stored command sequences, and system status information. The CD&H implements an external watchdog, implemented within the EPS and described in more detail below, for latch-up mitigation and internally tracks system state history to aid operational recovery from inadvertent resets. The MSU-designed Space Flight Computer (SFC) normally contains a 64-Gb (8-GByte) NAND flash storage for bus and payload data. The RAS payload operates at significantly higher data rates than the particle detectors on FIREBIRD, yet the dual processors have ample margin for processor load and memory utilization. The RAS camera data rate is ~30 to 60 Mbps while recording a scene, so a 20-second long scene could easily produce a 1-Gb downlink file if the full high-speed video is stored on board for later transmission. Mitigations for this are discussed below. The video will likely be processed and stored in the payload module.

Flight Software

The flight software design also leverages FIREBIRD/IT SPINS heritage code. The flight software has the ability to store and execute command sequences that are time-tagged for boot-up, spacecraft/payload commissioning and normal mission operations. Command tables are initially loaded before launch and can be uploaded and saved for future execution during the mission based on time or telemetry cues. C&DH flight software is implemented in the C language as an application in the Micrium µC/OS-II operating system. The flight software is designed to be highly modular and configurable.

On each boot-up, the flight software executes the first stored sequence in memory. This boot sequence configures the spacecraft by executing other configuration sequences. If a change to the spacecraft configuration needs to be made on-orbit, a replacement sequence may be uploaded for execution on subsequent boots.

Another significant part of the C&DH flight software is the telemetry monitor (TLMMON) module, which allows alarm limits to be set for specific telemetry points. If the alarm is exceeded a command sequence may be started or halted, depending on the configuration. The TLMMON is used to enter safe mode if the battery voltages drops too low and end GPS data runs if the GPS temperature exceeds a critical limit. The TLMMON module relies heavily on the telemetry manager (TLMMGR) module, which is responsible for routing all telemetry within the spacecraft. When new telemetry is received from a

subsystem, the TLMMGR will route it to the configured output, such as COMM, the Ground Support Equipment (GSE) port, or memory. The TLMMGR is also used to route telemetry to specific outputs at a configured cadence. This timed telemetry configuration is used to control the RF beacon.

Electrical Power System (EPS)

The EPS requirements are generally similar to other small satellites, although with the unique requirement to support SARAS experiments. The EPS system consists of solar panels, Li-ion batteries and a power storage and distribution system which evolved at MSU through the FIREBIRD and IT SPINS developments. This so-called Phoenix EPS is based on a direct energy-transfer system; the battery pack is directly connected to the solar arrays via protection diodes. RASSat's body-mounted panels host 27 Emcore triple-junction cells that, in turn, charge a set of two Li-ion batteries to supply the spacecraft with 8.4 V of unregulated power. The EPS provides two switchable 3.3V and 5V rails in addition to three switchable unregulated bus lines and disables all spacecraft loads until the required 30-min period after ejection from the carrier/deployer system.

The power control utilizes relatively straightforward, high-efficiency, direct energy transfer from all four solar array inputs and has a shunt to dissipate excess energy in the system while operating in conjunction with battery charge regulators and overcharge protection. The latter circuit disconnects the battery cells from the system bus whenever the bus exceeds a set voltage. If the battery is fully charged and the solar arrays are still providing power, the batteries will be disconnected from the system and the solar array will power the entire spacecraft.

Another key feature of the Phoenix EPS is the hardware WatchDog Timer (WDT). This WDT is implemented using basic logic gates that count up to 12 hours then power cycle the entire spacecraft for 10 seconds. This 12-hour reset is used to resolve any single-event upsets due to radiation strikes or software bugs.

The SARAS circuitry interfaces directly to the solar arrays, is self-powered and produces multichannel audio signals along with low rate-data recovery, both of which are passed to the RAS experiment package. SARAS is sensitive to internal spacecraft audio-frequency vibrations as may be caused by momentum wheels. An experiment goal is also to quantify susceptibility to audio-frequency EMI including modulated RF.

A refined electrical power budget for RASSat has yet to be generated, but in approximate terms the RAS sensor payload module will draw ~2 Watts during standby and ~3.5 watts during signal acquisition and recording. Other significant power use will likely be from the ADCS (~1.5 to 3.5 Watts) and downlink transmitter (~2-3 Watts).

Communication Subsystem (COMM)

Sensor module data will drive the RASSat COMM performance requirements. The RAS payload generates high-definition 1080p30 or 720p30 video stream with compressed stereo audio at 30 to 60 Mbps and with a typical 30-second scene recording duration. The data is stored locally in the sensor payload module producing a 1-Gb scene data file. This data size can be reduced by reducing the frame rate and image size. Reducing 30 fps to 3 fps, cropping to a 25% image area and shortening the scene to 10 seconds would reduce the file size by a factor of 120; thus, 8.3 Mb of video plus 1.28 Mb of RAS audio (10 seconds of single channel RAS data at 8 Ksps/16 bit resolution) would need to be downlinked. The RAS detector can produce four audio channels with 24-bit resolution at a 48-KHz sample rate (4.6 Mbps). For the demonstration mission described here this could significantly be reduced down to one RAS channel at 8 KHz/16-bit resolution (128 Kbps) and even further if compressed.

The heritage communications subsystem comprises an AstroDev Lithium UHF half-duplex radio operated at 19.2 kbps and a UHF-deployed dipole. This radio is at TRL 9, having been successfully used on numerous CubeSat missions. A preliminary link budget using MSU's existing ground station and a 1W transmitter on the spacecraft (see Table 4) concludes there is sufficient power margin for both the uplink and downlink. This setup has been demonstrated to work nominally during FIREBIRD mission operations. This transmitter could downlink a 8.3 Mb file in 7.2 minutes. But other radios such as S-band should be considered so as to return a more complete data set. Higher bandwidth transmitters capable of supporting operational RASSat missions include the SpaceQuest TX-2400M S-Band transmitter (up to 5.6 Mbps) and the TUI SWIFT™ family of software-defined radios operating at either UHF or S-band frequencies.

Attitude Determination and Control Subsystem (ADCS)

RASSAT must be able to point and track fixed or slowly moving objects on Earth's surface during an overflight. ADCS requirements are similar to other medium-resolution optical remote-sensing satellites. The RASSat camera horizontal field of view is 0.34° (2.4 km) with a 0.23° (1.6 km) RAS field of view. The spacecraft should ideally be able to point an order of magnitude better providing a peak georeferenced pointing error on the order of 0.023° (~160 m). The RASSat ADCS pointing and control requirements are met by the Blue Canyon Technologies' 0.5U XACT 3-axis, stellar based CubeSat ADCS[22] (see Fig 9), capable of providing better than 0.007° pointing accuracy in each of 3-axes and has a slew rate capability of >10°/second. The XACT star-tracker-based system masses at 0.91 kg and uses 2-3 Watts (mode-dependent) in operation.

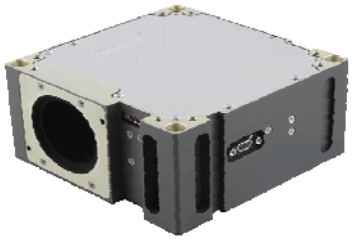

Figure 9: Blue Canyon Technologies XACT ADCS module meets the pointing and slew rate requirements of the RASSat mission.

RASSAT MISSION DESIGN

For this paper, the baseline mission design is assumed to be for a RASSat technology-demonstration mission in LEO, starting with RASSat deployment from the ISS via the well-proven pathway to orbit offered by Nanoracks. The RASSat Mission Control Center is assumed to be at MSU (~40 deg. North latitude). Such an orbit (and orbit lifetime) satisfies the top-level RASSat mission and system objectives defined above.

For the initial tech-demo mission design, several RAS observing scenarios were defined to facilitate further mission analysis:

- Repeatedly observe two specific geographic locations on the ground, one featuring natural phenomena of interest and the other human-made phenomena. The respective locations chosen were Mauna Loa in Hawaii (occasionally experiencing active eruptions and lava flows) and Disneyland in Anaheim, California (featuring ~15-minute fireworks shows every evening at 9:30).
- Repeatedly observe locations on water surfaces where the glint from the reflected disc of the Sun can be captured.
- Observe other space objects (e.g., ISS) on a targets-of-opportunity to better characterize RAS for SSA applications.

Observations of Terrestrial Phenomena

Commissioning of the spacecraft will consume no more than three weeks. Following this initial check-out phase, a nominal 6-month primary mission duration is assumed. Should orbital-lifetime predictions support it, an extended mission phase of a few weeks or months could be considered.

We modeled a typical orbit achieved after an ISS CubeSat deployment: a circular orbit that decayed from 415 km altitude to 365 km altitude in six months, covering +/- 51.6 deg. latitude every 92-minute orbit. We modeled our orbits based on actual CubeSat deployments from the Nanoracks launcher during July, 2015.

Although the satellite has line-of-sight access to the targets, we constrained valid access to those that were in an average 0.25 deg. field of view, at least 30 seconds long, had the satellite at least 45 deg. above the horizon, and had the target no more than 45 deg. off nadir. We also constrained the maximum slew rate to 10 deg./second (although the maximum we saw was about 5 deg./second). When constrained that the target sites must be in direct sunlight, over a six-month period (see Fig. 10) there were about 64 times the RAS sensor could collect on Mauna Loa, HI and about 80 on Anaheim, CA. (These results are from a point solution, and would vary somewhat with different initial conditions when leaving the ISS.) The results are similar when the targets are constrained to be in penumbra or umbra (Fig. 11), with 66 collect opportunities on Mauna Loa and 96 on Anaheim.

When looking at the Sun's glint off a body of water, there are fewer opportunities than simple observation because the angle from the camera off the surface to the Sun has to be so precise. We looked at glints from the Chesapeake Bay (about 4,500 square miles) and from Lake Huron (about 23,000 square miles). With collections constrained to a minimum duration of 10 seconds, over 6 months there were 13 times to observe the glint on the Chesapeake Bay, and 120 opportunities to observe on Lake Huron (Fig. 12).

Table 4. RASSat downlink power budget.

Parameter	Nominal	Favorable	Adverse
Frequency (MHz)	437.000	437.000	437.000
Distance (km)	600.000	400.000	1000.000
Transmitter power (dBm)	30.000	34.000	28.000
Antenna circuit loss (dB)	-1.000	-1.000	-1.000
Antenna gain (dBi)	3.000	3.000	3.000
Antenna pointing loss (dB)	-6.000	-6.000	-6.000
EIRP (dBm)	26.000	30.000	24.000
Free space loss (dB)	-140.820	-137.299	-145.257
Atmospheric attenuation (dB)	-0.600	-0.400	-1.000
Receive power density (dBm/m^2)	-115.420	-107.699	-122.257
Polarization loss (dB)	-3.000	-3.000	-3.000
Receive antenna gain (dBi)	18.000	22.000	16.000
Pointing loss (dB)	0.000	0.000	0.000
Receiver circuit loss (dB)	-1.000	-1.000	-1.000
Receiver input (dBm)	-101.420	-89.699	-110.257
Noise spectral density (No) (dBm/Hz)	-174.000	-184.400	-164.000
Channel bandwidth (Hz)	25000	25000	25000
Channel noise power (dBm)	-130.021	-140.421	-120.021
Channel SNR (dB)	28.600	50.722	9.763
Shannon channel capacity (bits/sec)	237569	421237	84702

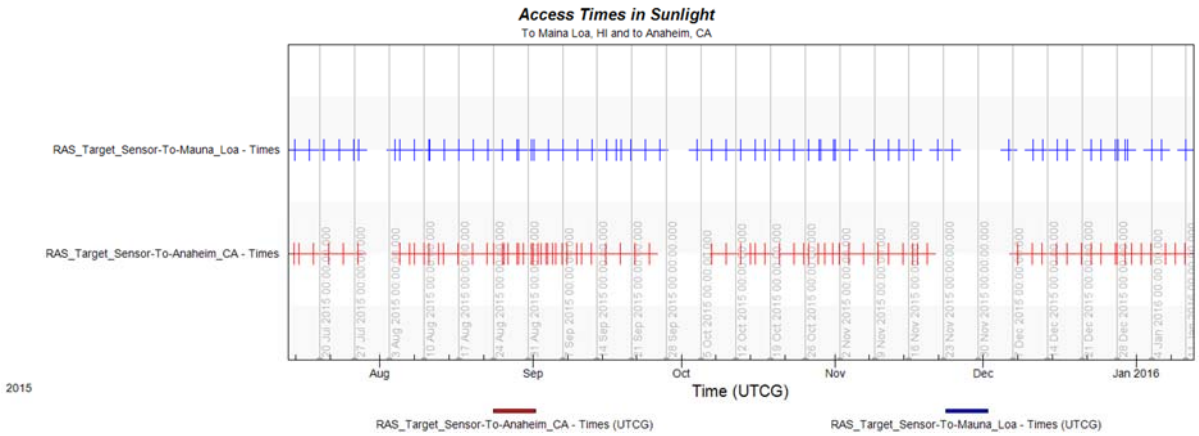

Figure 10: RAS observation opportunities over a 6-month period for Mauna Loa, HI and Anaheim, CA (targets in sunlight).

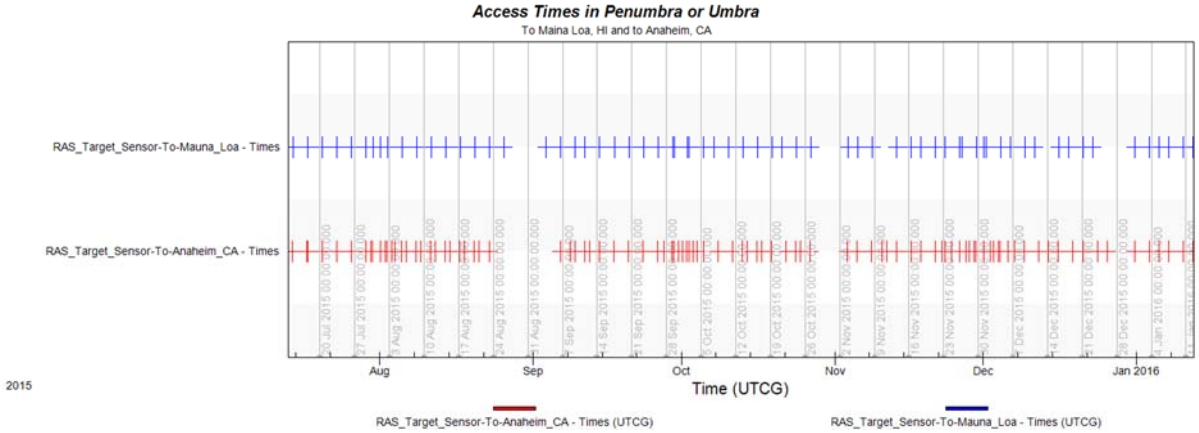

Figure 11: RAS observation opportunities over a 6-month period for Mauna Loa, HI and Anaheim, CA (targets in darkness or dawn/dusk).

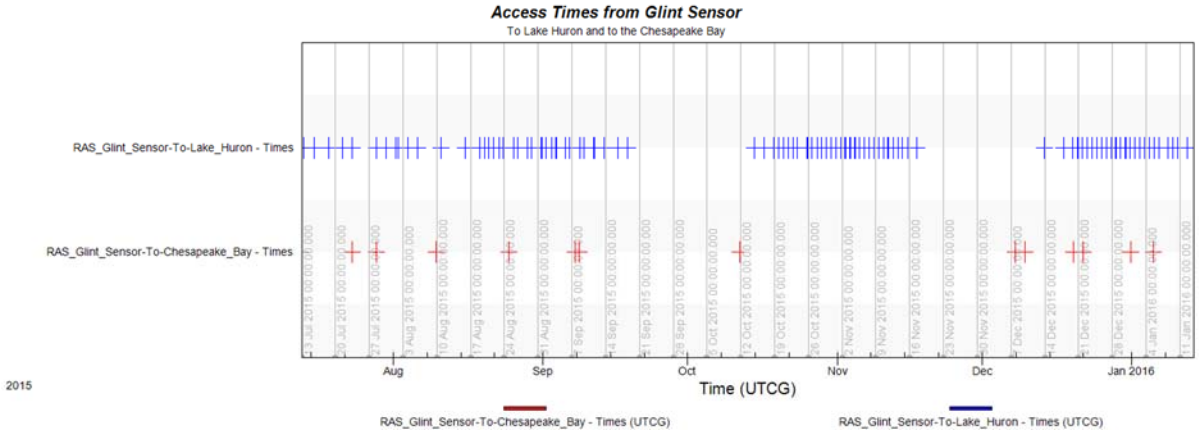

Figure 12: RAS observation opportunities over a 6-month period for water surface Sun-glint experiments.

Observations Supporting Space Situational Awareness

SSA is the requisite knowledge to predict, deter, avoid, operate through, recover from, and/or attribute cause to the loss, disruption, and/or degradation of space services and capabilities. A main objective of SSA is to provide decision-making processes with a timely and accurate body of evidence of space object and event related behavior(s) attributable to space threats and hazards. To meet and satisfy SSA needs, the rigorous and comprehensive detection, tracking, identification, characterization, and classification of space objects and events is desired. At present, most space objects and events are understood in terms of their location and effect, and some of these are understood in terms of their physical characteristics as inferred from radars and telescopes.

The fluctuation of reflected or emitted radiation of space objects is currently used for detection, tracking, identification, characterization, and classification. If this is photon scatter, the term "light curve" or more technically, photometry, is typically used for the time-history of the observed photon flux. Photometric signatures tend to be collected at a rate of 1 Hz. This provides insight into space object size, shape, orientation, and material properties but is extremely challenging because a large invers problem needs to be solved.

If the photometry is collected hypertemporally (e.g. ~40 KHz), the information content in the light curve could then be converted into an equivalent mechanical wave (acoustic signature) which the human brain is good at characterizing with more refinement than optical signatures alone. Thus, the potential benefit of RAS derives from the development and maintenance of a database on all detectable space objects in terms of this acousto-optic signature. The specifics of how space objects behave as an interpreted sound could provide an order-of-magnitude or greater richness with which to uniquely identify, describe, and predict them and their behavior against threat and hazard risks. Moreover, this acousto-optic characterization and classification would allow for more rapid and meaningful detection and tracking in the presence of unresolved data.

The University of Arizona's Space Object Behavioral Sciences (SOBS) initiative[23] is attempting to quantify the Earth-orbiting human-made space object population as an ecosystem populated with classes and species of space objects, and this acousto-optic signature could be used as a form of class/specie-dependent fingerprint to further aid in the development of scientific taxonomies of this population. To demonstrate and validate the value of RAS in this arena, targets of opportunity would be defined as part of the mission-design process, building windows of time into the observational plan to allow for pointing RASSat's sensors at objects of interest such as ISS, arriving/departing ISS cargo and crew vehicles, other LEO satellites passing at relatively close range, re-entering objects, rockets ascending from launch to orbit, etc. Each observation would be new and pathfinding and would add to the overall SSA database.

RASSAT INTEGRATION, TESTING AND LAUNCH OPERATIONS

The RASSat sensor payload module will be fully integrated and tested (functionally and environmentally) before its integration with the RASSat bus. Flight qualification of the RASSat payload module requires optical testing in addition to the usual thermal, vacuum, vibration and electromagnetic compatibility testing. A visual/aural scene generator operating either with collimation optics or in a far-field mode produces calibrated sensor stimuli, and special test equipment and bus emulators serve to check out and validate payload-to-bus interfaces.

Integration and testing of the RASSat bus involve a process now very typical for 3U CubeSats, i.e., considerable subsystem and system-level functional tests in a 'flat-sat' arrangement, followed by system integration, system-level vibration and thermal-cycling tests, sometimes thermal-vacuum tests, various RF and sensor-calibration tests, and often one or more 'Day-in-the-life' tests.

Likewise, it is assumed here that the launch process would involve a proven method for getting 3U CubeSats into orbit, such as that routinely demonstrated by Nanoracks for placing CubeSats into the ISS orbit by deploying them from the end of the ISS robotic arm following transfer to ISS onboard a scheduled cargo resupply vehicle.

EXPECTED NEAR-TERM RASSAT DEVELOPMENT

Prior to launch of the RASSat 3U CubeSat, several space or near-space demonstrations can be performed to demonstrate the RAS capability and develop the capability to quantitatively interpret the aural signals.

The RAS sensor will be flown on a stratospheric balloon to ~100,000 ft. in summer 2016. The sensor will look upward, viewing the balloon envelope, which at altitude constitutes a huge diaphragm, intercepting pressure variations from both natural and anthropomorphic sources. A four-channel RAS sensor with each channel trained on a different azimuthal sector of the balloon envelope (red square target areas in Fig. 13) might even provide crude directional or stereophonic discrimination.

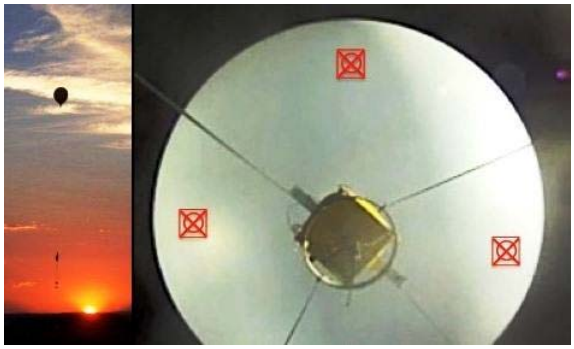

Fig 13. Typical camera view of stratospheric balloon envelope from gondola, with typical RAS targets in red.

Employing a RAS modified handheld high-definition camera for operation by the astronauts within the ISS is also being pursued, though 2017 is a more likely timeframe for such activity. A high-priority objective is to have the astronauts use RAS while in the ISS cupola to capture views of exterior ISS activity, terrestrial targets and in-space targets of opportunity.

CONCLUSIONS

This paper has provided a brief overview of remote acoustic sensing (RAS) technology as a possible tool for remotely listening to planetary surface sounds from an orbiting spacecraft. RASSat simulator experiments to date have shown that meaningful RASSat demonstrations could be performed cost effectively using a 3U CubeSat form factor. A next step would be to operate a RAS technology demonstrator on an orbiting spacecraft such as the ISS or build the actual RASSat spacecraft that we have described herein.

As in other imaging systems, larger telescope apertures will provide better acoustic detectability and resolution of more distant objects. Some of the stronger RAS signals such as lightning, fireworks and certain cultural activity should be readily observable even with the small RASSat. More sounds could be heard with a larger telescope typical of the small 1-m class Earth-imaging satellites such as those produced by Terra Bella (formerly Skybox Imaging). Another development option would be to add a RAS module to Terra Bella or other similar existing Earth remote-sensing satellites having video capabilities. Likely observable natural sounds include lightning, sprites, meteors, breaking ice flows, waterfalls, ocean surf and forest fires. Possibly observable natural sounds may include volcanos, aurorae, tornadoes, extreme weather, insect and bird swarms. Likely observable cultural sounds include city lights, fireworks, aircraft and other vehicle beacons and military activity. Possibly acoustically observable are vehicles, crowds, spinning objects, air and water flow, ship wakes, airports, amusement parks and similar.

RASSat simulator observations of more scenarios can help to further identify and quantify on-orbit RAS observability. Future sensitivity and capability enhancements are possible using larger optics, more sensitive detectors operating in more wavelength regions, more advanced SARAS capabilities along with improved signal processing including multichannel beamforming and multispectral acoustic sensing.

Although this paper has focused on terrestrial acoustic observations from an orbiting spacecraft we believe that there are potentially interesting RAS applications in the exploration of other worlds[1]. Sounds of other worlds may include Martian dust devils and surface flows of boiling water, Jovian lightning storms and aurorae, Io volcano plumes, Saturn ring motions, Enceladus plumes and Sun glints off Titan's hydrocarbon lakes. We have already applied RAS to listening to the sounds of protozoa living in microscopic aquatic worlds, and there found new sounds that have never been heard before. Thus, both macro-scale and microscopic RAS may prove useful on planetary landers. Planetary rovers augmented with RAS and SARAS could listen to weather conditions including wind flow and turbulence, twisters, lightning, aurorae, rain and fluid sounds as well as locally generated rover sounds caused by locomotion, gimbal drive motions, vortex shedding and sample acquisition operations. Microscopic RAS technology on planetary landers may prove useful for the detection and characterization of life on -- or in -- other worlds.

Certain aspects of RAS and SARAS are patented or pending.

ACKNOWLEDGMENTS

The lead author would like to thank Sandy Slater, M.D. for unwavering support of RAS development activities. We would also like to thank Joe Carroll of Tether Applications for seeing the aerospace potential of remote acoustic sensing and introducing several of the collaborators on this paper in the fall of 2014, thus initiating the collaboration summarized herein.

REFERENCES

1. Slater, D. and R. Ridenoure, "Passive Remote Acoustic Sensing in Aerospace Environments, "AIAA SPACE Forum 2015, Pasadena, CA (2015).
2. Slater, D., "A Telescopic Cinema Sound Camera for Observing High-Altitude Aerospace Vehicles," Proc. SPIE 9227, Unconventional Imaging and Wavefront Sensing 2014, 92270A (September 18, 2014); doi:10.1117/12.2061399.
3. Bell, A.G., "Apparatus for Signaling and Communication, Called Photophone," US patent 235,199 (1880).
4. Bell, A.G., "Photophone Transmitter," US patent 235,496 (1880).
5. Bell, A.G., "On the Production and Reproduction of Sound by Light," American Journal of Sciences, Third Series, vol. XX, no. 118, Oct. 1880, pp. 305-324.
6. Bell, A.G., "Photophone Receiver," US patent 241,909 (1881).
7. Bell, A.G., "Transmitting and Recording Sounds by Radiant Energy," US patent 341,213 (1886).
8. Davis, et. al., "The Visual Microphone: Passive Recovery of Sound from Video," ACM Transactions on Graphics (Proc. SIGGRAPH), 2014 vol 33 # 4 79:1-79:10.
9. Clark, F. O., R. Penney, W. E. Pereira, J. Kielkopf and J. Cline, "A Passive Optical Technique to Measure Physical Properties of a Vibrating Surface," Proc. SPIE 9219, Infrared Remote Sensing and Instrumentation XXII, 92190G (September 12, 2014).
10. Marchant, A., C. Fish, J. Yao, P. M. Cunio and W. E. Pereira, "Feasibility Considerations for a Long-Range Passive Vibrometer," Proc. SPIE 9219, Infrared Remote Sensing and Instrumentation XXII, 92190F (September 12, 2014).
11. Slater, D., "Passive Long-Range Acoustic Sensor," US patent 7,551,519 (June 23, 2009).
12. Slater, D. and S. Shaw Slater, "Remote Sensing with Passive Specular Probes," Proc. SPIE 6709, Free-Space Laser Communications VII, 67090W (September 25, 2007); doi:10.1117/12.734838.
13. Slater, D., "Passive Long-Range Acousto-Optic Sensor, "Proc. SPIE 6304, Free-Space Laser Communications VI, 63040E (September 01, 2006); doi:10.1117/12.681389.
14. Tsitas, S. R. and J. Kingston, "6U CubeSat Design for Earth Observation with 6.5m GSD, Five Spectral Bands and 14Mbps Downlink," The Aeronautical Journal, November 2010, vol. 114 no. 1161 689.
15. Verdone, P., "A Telescope Suitable for Rocket-Borne Instrumentation," NASA Goddard Space Flight Center, November 1966.
16. Boshuizen, C. R., J Mason, P. Klupar and S. Spanhake, "Results from the Planet Labs Flock Constellation," 28th Annual AIAA/USU Conference on Small Satellites, Logan, Utah (2014).
17. Iizuka and Yutaka, "Catadioptric Telephoto Lens," US patent 4,666,259 (February 26, 1985).
18. For more information see Ecliptic's website, www.eclipticenterprises.com.
19. Ridenoure, R., et. al, "LightSail Program Status: One Down, One to Go," Paper SSC15-V-03, 29th Annual AIAA/USU Conference on Small Satellites, Logan, Utah (2015).
20. Klumpar, D.M., et al., "Flight System Technologies Enabling the Twin-CubeSat FIREBIRD-II Scientific Mission," Paper SSC15-V-06, 29th Annual AIAA/USU Conference on Small Satellites, Logan, Utah (2015).
21. See https://ssel.montana.edu/itspins.html.
22. See http://bluecanyontech.com/portfolio-posts/attitude-control-systems/.
23. See http://sobs.arizona.edu.